Interaction between 6-Hydroxydopamine and Transferrin: "Let My Iron Go"†

Grigory G. Borisenko,*,‡ Valerian E. Kagan,*,‡,§ Carleton J. C. Hsia,|| and Nina Felice Schor⊥

Department of Environmental and Occupational Health, Department of Pharmacology, and Department of Pediatrics and Neurology, University of Pittsburgh, Pittsburgh, Pennsylvania 15238, and SynZyme Technology, LLC, Irvine, California 92618

Received October 4, 1999; Revised Manuscript Received December 16, 1999

ABSTRACT: The dopamine analogue 6-hydroxydopamine (6-OHDA) is selectively toxic to catecholaminergic neurons. Because of its selectivity for neuroblastic cells in the sympathetic nervous system lineage, 6-OHDA has been suggested as a chemotherapeutic agent for targeted treatment of patients with neuroblastoma. We tested the hypothesis that the toxicity of 6-OHDA is caused by its interaction with serum ferric transferrin (Fe-TF) resulting in release of iron. We further hypothesized that this iron, through its redox-cycling by 6-OHDA, triggers generation of reactive oxygen species. 6-OHDA-induced release of iron from Fe-TF was demonstrated by: (1) low-temperature EPR spectroscopic evidence for decay of the characteristic Fe-TF signal ($g = 4.3$) and appearance of the high-spin signal from iron chelated by 6-OHDA oxidation products; (2) spectrophotometric detection of complexing of iron with the Fe^{2+} chelator ferrozine; (3) redox-cycling of ascorbate yielding EPR-detectable ascorbate radicals; and (4) generation of hydroxyl radicals as evidenced by EPR spectroscopy of their adduct with a spin trap, 5,5′-dimethylpyrroline oxide (DMPO) (DMPO-OH). Our low-temperature EPR studies showed that in human plasma, 6-OHDA caused iron release only under nitrogen gas but not under air or oxygen. The absence of a 6-OHDA effect in plasma under aerobic conditions was most likely due to its ferroxidase activity [with consequent reuptake of Fe(III) by apoTF] and catalytic oxidation of 6-OHDA by ceruloplasmin. Modeling of these plasma activities by a stable nitroxide radical, 2,2,6,6-tetramethyl-1-piperidinyloxy (TEMPOL), resulted in protection of plasma Fe-TF against iron release under nitrogen. Parenteral administration of 6-OHDA to mice resulted in iron release from Fe-TF as evidenced by transformation of the Fe-TF low-temperature EPR signal that was indistinguishable from that seen in in vitro models. In addition, administration of the iron chelator deferoxamine (DFO) to mice prior to administration of toxic doses of 6-OHDA resulted in a decrease in activity impairment of mice as compared to that seen with 6-OHDA alone. These findings underscore the physiological and pharmacological relevance of 6-OHDA-mediated iron release from Fe-TF and suggest that iron chelators (DFO) may be used for prevention of 6-OHDA toxicity.

The dopamine analogue 6-hydroxydopamine (6-OHDA)[1] is selectively toxic to catecholaminergic neurons. This compound has been used to develop animal models for the study of Parkinson's disease, a disorder in which the long-term toxicity of dopamine and its breakdown products has been hypothesized to play a pathogenetic role (*1*). Furthermore, because of its selectivity for neuroblastic cells in the sympathetic nervous system lineage, 6-OHDA has been suggested as a chemotherapeutic agent for targeted treatment of patients with neuroblastoma (*2*−*4*). The toxic effects of 6-OHDA are largely related to its ability to generate superoxide radicals and hydrogen peroxide. OHDA is readily oxidized to the corresponding *p*-quinone in the presence of molecular oxygen. In this process, each of two molecules of oxygen accepts an electron from 6-OHDA (denoted as the dihydroquinone, QH_2) in this series of reactions:

$$QH_2 + O_2 \rightleftharpoons {}^{\bullet}QH + O_2^{\bullet-} + H^+ \quad (1)$$

$${}^{\bullet}QH + O_2 \rightleftharpoons Q + O_2^{\bullet-} + H^+ \quad (2)$$

The superoxide radical thus generated promotes further oxidation of 6-OHDA by accepting an electron in the following reaction (*5*):

$$QH_2 + O_2^{\bullet-} + H^+ \rightleftharpoons {}^{\bullet}QH + H_2O_2 \quad (3)$$

Studies aimed at modeling the pathogenesis of Parkinson's disease demonstrated that 6-OHDA is highly effective in releasing iron as Fe(II) from ferritin (*6*). This is important because iron may catalytically accelerate reaction 1, the rate-limiting step in oxidation of 6-OHDA (*7*), i.e., enhance subsequent production of H_2O_2 and $O_2^{\bullet-}$. In addition, Fe(II)

† This research was supported by the NIH (SBIR Grant CA79378 and Grant R01 CA74289) and by the American Institute for Cancer Research (Grant 97B128).

* All correspondence should be addressed to either of these authors at the Department of Environmental and Occupational Health, University of Pittsburgh, 260 Kappa Dr., Pittsburgh, PA 15238. Phone: (412) 967-6561 (G.G.B.) or (412) 967-6516 (V.E.K.). Fax: (412) 624-1020 (G.G.B. and V.E.K.). E-mail: grigoryb@yahoo.com (G.G.B.) or kagan+@pitt.edu (V.E.K.).

‡ Department of Environmental and Occupational Health.

§ Department of Pharmacology.

|| SynZyme Technology.

⊥ Department of Pediatrics and Neurology.

[1] Abbreviations: 6-OHDA, 6-hydroxydopamine; DFO, deferoxamine; TEMPOL, 4-hydroxy-2,2,6,6-tetramethyl-1-piperidinyloxy; CP, ceruloplasmin; DMPO, 5,5-dimethyl-1-pyrroline *N*-oxide; TF, transferrin; apoTF, apotransferrin; Fe-TF, ferric transferrin.

10.1021/bi992296v CCC: $19.00
Published on Web 03/21/2000

released from ferritin can react with H_2O_2 to produce the highly toxic hydroxyl radical ($^{\bullet}OH$).

Undoubtedly related to this endogenously propagated generation of highly reactive radical species, treatment of tumor-bearing mice with 6-OHDA is found to be toxic not only for the neuroblastoma cells of the tumor but systemically as well (*3*). This is not surprising, since, in tissues without a cellular catecholamine uptake system, parenterally administered 6-OHDA (and reactive oxygen species generated) would be expected to react with extracellular targets.

One such potential target is serum transferrin (TF), a major carrier and storage protein of iron. ApoTF contains two metal-binding sites which form high-affinity complexes with ferric ion (*8*). This iron can be liberated by a number of reducing agents, including hydroxypyridonates and catechols (*9*). We hypothesized that 6-OHDA, a catecholamine, can reduce and release iron from TF. Iron liberated from TF would perpetuate formation of reactive oxygen species that would in turn perpetuate the release of iron from TF.

Some existing lines of evidence have been interpreted as arguing against this hypothesis. Previous studies suggest that diferric transferrin does not in fact accelerate $^{\bullet}OH$ formation (*10*) from superoxide (generated by the xanthine−xanthine oxidase system) and hydrogen peroxide. Superoxide may not cause iron release except at acidic pH or TF iron saturation levels above those seen physiologically (*11*). Finally, incubation of TF with plasma does not alter the intensity of the ascorbate radical EPR signal generated from ascorbate except when the added iron concentration exceeds the iron-binding capacity of plasma (*12*). It is of interest that all of these studies involved biochemical systems containing H_2O_2 or $O_2^{\bullet-}$ in the absence of reducing agents. This situation may differ markedly from that of systems containing 6-OHDA or dopamine, redox-cycling reductants that perpetuate ongoing release of iron as well as H_2O_2 and $O_2^{\bullet-}$ production. The present study examines a system containing both TF and 6-OHDA. It demonstrates the prooxidant role of transferrin in such systems and suggests a novel additional mechanism for 6-OHDA toxicity. We demonstrate the iron-releasing effect of 6-OHDA on TF, assess the importance of this phenomenon in vivo, and suggest its relevance for iron redox cycling and oxygen radical generation in disease and therapy of the nervous system.

METHODS

Reagents. Human serum apotransferrin (apoTF), human ceruloplasmin (CP), 6-OHDA, ferrous sulfate, sodium ascorbate, 4-hydroxy-2,2,6,6-tetramethyl-1-piperidinyloxy (TEMPOL), 3-(2-pyridyl)-5,6-bis(4-phenylsulfonic acid)-1,2,4-triazine (ferrozine), and deferoxamine were purchased from Sigma Chemical Co. (St. Louis, MO). 5,5-Dimethyl-1-pyrroline *N*-oxide was obtained from Aldrich Chemical Co. (Milwaukee, WI). Trisma base and Tris-HCl were purchased from Bethesda Research Laboratories. Compressed nitrogen gas (>99.9% purity) and oxygen gas were obtained from Valley Welding (Pittsburgh, PA). Plasma was obtained from heparinized blood of anonymous healthy donors by centrifugation for 20 min at 1500*g*.

Animals. Male A/J mice were obtained from The Jackson Laboratory (Bar Harbor, ME) at 5−7 weeks of age. Mice were housed four per cage and given free access to food and water throughout the experiment. In all cases, they were acclimated to the animal facility for at least 72 h prior to use.

Fe-TF Preparation. ApoTF (25 μM) was loaded with iron up to 30, 60, and 90% saturation by addition of varying amounts of $FeSO_4$ in the presence of CP (0.4 unit/mL). Incubations were carried out in Tris buffer, 10 mM, pH 7.4, for 1 h. This low concentration of CP was used to avoid CP-dependent oxidation of 6-OHDA in subsequent incubations (*13*). Optical density measurements of Fe-TF complexes [characteristic maximum $\epsilon_{465} = 4950\ M^{-1}\ cm^{-1}$ (*14*)] or low-temperature EPR measurements of the typical Fe-TF spectrum were used for close monitoring and control of the binding capacity of apoTF and the saturation level of Fe-TF. A 90% saturation of Fe-TF occurred within 2 min incubation of apoTF in the presence of $FeSO_4$ and CP.

Treatment of Plasma and Fe-TF in Buffer for Low-Temperature EPR Measurements of Fe-TF. The concentrations of 6-OHDA used for these in vitro studies were chosen because they are readily attained in the serum of animals given parenteral 6-OHDA (*3*) and in neural crest cells incubated with this compound (*15*). In accordance with this, 6-OHDA (4 mM) was added to Fe-TF (20 μM) and CP (0.4 unit/mL) in Tris buffer, 10 mM, pH 7.4. After various periods of time, samples were frozen in liquid nitrogen for subsequent analysis. Samples of plasma were frozen immediately for Fe-TF measurements, after addition of exogenous Fe to evaluate the endogenous level of iron saturation of TF, or after treatment with 6-OHDA (4 mM). Incubations of plasma with 6-OHDA were carried out for 1.5 h in equilibrium with air, or under flow of pure O_2 or N_2. Plasma was partially evaporated during incubation, and its volume was restored with Tris buffer (10 mM, pH 7.4) maintained under the same flow of gas. EPR measurements of the Fe-TF signal were performed on a JEOL-RE1X spectrometer under the following conditions: 150 mT, center field; 80 mT, sweep width; 1 mT, field modulation; 10 mW, microwave power; 0.3 s, time constant; 2 min, time scan; 77 K, temperature.

EPR Measurement of Ascorbate Radical. Redox activity of iron was evaluated by measurement of ascorbate radical production. Fe-TF (25 μM, about 85% saturation), apoTF (25 μM), or Fe(II) was incubated for 2 h with 6-OHDA (4 mM). The catecholamine was similarly incubated alone as a control. CP (0.4 unit/mL) used for loading TF with iron was added to all incubations to make the conditions comparable. Immediately after treatment, samples were diluted 8-fold for ascorbate radical measurement. The diluent contained ascorbate (500 μM), SOD (10 μM), and 6-OHDA (500 μM). Control (i.e., not treated with 6-OHDA) aliquots of apoTF and Fe-TF were similarly analyzed in parallel. Ascorbate radical spectra were recorded with the following settings: 335.4 mT, center field; 0.5 mT, sweep width; 0.063 mT, field modulation; 10 mW, microwave power; 0.1 s, time constant; 1 min, time scan. Time courses of ascorbate radical ESR measurements were obtained by repeated scanning of the magnetic field corresponding to the low-field peak of the ascorbate radical spectrum. These records were then transformed into a plot of the time course of signal magnitude by plotting the peak of the EPR signal at each time point. The inflection time of ascorbate radical generation was defined as that point on the time course at which the rate of increase in amplitude of the EPR signal was maximal. The

conditions for these measurements (internal mode of recording) were as above except that the sweep width was 0.15 mT and the time scan was 10 s.

EPR Measurements of Hydroxyl Radical Adduct with a Spin Trap, DMPO (DMPO−OH). Measurements of DMPO−OH production were carried out in the presence of DMPO (100 mM) and 6-OHDA (500 μM) after addition of apoTF (2.5 μM), 85% saturated Fe-TF (2.5 μM), or $FeSO_4$ (5 μM). Spectra of the DMPO−OH adduct were recorded at 335.4 mT, center field; 4 mT, sweep width; 0.1 mT, field modulation; 10 mW, microwave power; 0.1 s, time constant; 1 min, time scan. Time courses of DMPO−OH adduct generation were obtained by repeated scanning of the magnetic field corresponding to one of the peaks of the EPR spectrum under the following conditions: 333.2 mT, center field; 0.3 mT, sweep width; 0.1 mT, field modulation; 10 mW, microwave power; 0.1 s, time constant; 10 s, time scan; internal mode of recording.

Fe(II)−ferrozine complex formation and 6-OHDA oxidation were monitored spectrophotometrically (Shimadzu UV160U spectrophotometer). For this purpose, Fe-TF (20 μM) was incubated for 2 h with 6-OHDA (4 mM) in the presence of CP (0.4 unit/mL) in Tris buffer, 10 mM, pH 7.4.

Effect of 6-OHDA on Fe-TF in Vivo. Mice were administered 6-OHDA (350 mg/kg in iced saline) or an equivalent volume of iced saline alone (control) by intraperitoneal injection. One hour later, they were anesthetized by brief halothane inhalation and sacrificed by cardiac puncture. Blood so obtained was collected in heparinized syringes and immediately frozen in liquid nitrogen for subsequent analysis.

Grading of Animals for Activity Level. Mice were administered deferoxamine (130 mg/kg) in normal saline or an equivalent volume of saline by intraperitoneal injection. Two hours later, 350 mg/kg of 6-OHDA (in iced saline) or an equivalent volume of iced saline was administered intraperitoneally. Animals were scored at various time points after injection for activity level, a measure of systemic well-being (*3*, *4*). Briefly, activity was graded using the following scale: 3, normal activity; 2, lethargic but ambulatory; 1, nonambulatory but alive; 0, dead. Determination of the statistical significance between treatment groups at the various time points was made using the Mann−Whitney U test for nonparametric data (*16*), and accepting a p value maximally 0.05 as indicative of statistical significance.

RESULTS

6-OHDA Releases Iron from Fe-TF. Figure 1, b shows the EPR spectrum of Fe-TF subsaturated with iron (90%) in the presence of CP. This characteristic signal corresponds to high-spin Fe(III) in TF. Addition of 6-OHDA to Fe-TF caused distinct transformation of the EPR signal over a 2 h period of incubation (Figure 1, c−e). The EPR signals of Fe-TF 60% or 30% saturated with iron underwent qualitatively similar but slower changes during incubation with 6-OHDA (data not shown). Thus, during incubation with 6-OHDA, the characteristic EPR signal of native Fe-TF (Figure 1, b) decreases in intensity and ultimately disappears, while a new signal emerges (Figure 1, f). Spectra obtained between 0 and 2 h after addition of 6-OHDA have the expected composite profiles reflecting the relative abundance of native and 6-OHDA-treated Fe-TF.

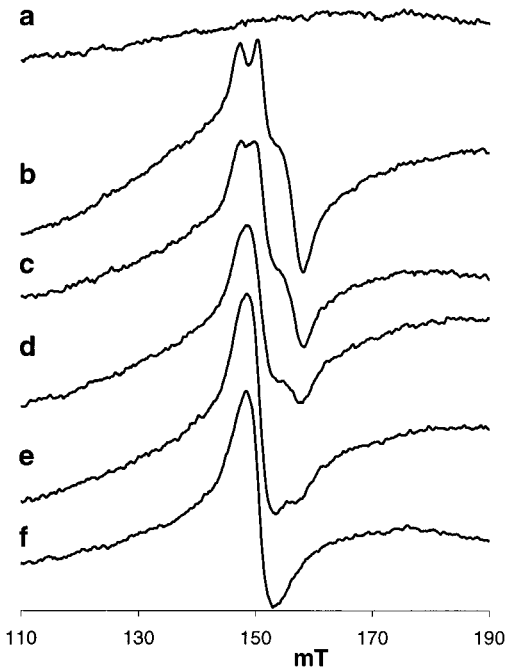

FIGURE 1: Effect of 6-OHDA on the low-temperature EPR spectrum of Fe-TF. (a) ApoTF (20 μM) in Tris buffer, 10 mM, pH 7.4; (b) Fe-TF (20 μM) 90% saturated with iron in the presence of CP (0.4 unit/mL); (c−e) same as "b" but in the presence of 6-OHDA (4 mM): spectra were recorded after 30 min, 1 h, and 2 h of incubation correspondingly; (f) $FeSO_4$ (40 μM) was incubated with 6-OHDA (4 mM) in Tris buffer, 10 mM, pH 7.4, for 2 h. All incubations were carried out at room temperature. Samples were then frozen in liquid nitrogen until measurements were made. Instrumental conditions: 150 mT, center field; 80 mT, sweep width; 1 mT, field modulation; 10 mW, microwave power; 0.3 s, time constant; 2 min, time scan; 77 K, temperature.

The emergence of the new signal may represent modification of Fe-TF complexes, which in turn could reflect oxygen radical-induced protein damage. That such modifications in protein structure can result in transformation of the EPR signal of Fe-TF is illustrated by the fact that the single-point tyrosine 95 mutant of the N-lobe of human TF has an EPR spectrum indistinguishable from that observed on incubation of Fe-TF with 6-OHDA (*17*). Alternatively, this signal can be associated with the release of iron from TF and formation of Fe(III) complexes with 6-OHDA oxidation products. Such oxidation products might be expected to complex with iron because they are aminophenols and have similar coordination chemistry to that of tyrosine. (Two tyrosines participate in the coordination of iron in the binding site of TF.) Furthermore, dopamine is also known to form complexes with Fe (*18*). Consistent with the notion of iron complex formation with 6-OHDA oxidation products, the same EPR signal was observed after incubation of iron (in the absence of TF) with 6-OHDA (Figure 1, f).

Direct demonstration of the 6-OHDA-induced release of iron by TF was achieved by filtration of Fe-TF and $FeSO_4$ solutions before and after treatment with 6-OHDA. Figure 2 shows the EPR spectra obtained from solutions of Fe-TF (left panel) and $FeSO_4$ (right panel). Both panels represent spectra recorded before (Figure 2, left and right, a) and after (Figure 2, left and right, b) treatment with 6-OHDA for 2 h. Both solutions gave the same signal after treatment. Treated samples were passed through 30 000 Da cutoff filters, and their EPR signals were again obtained (Figure 2, left and

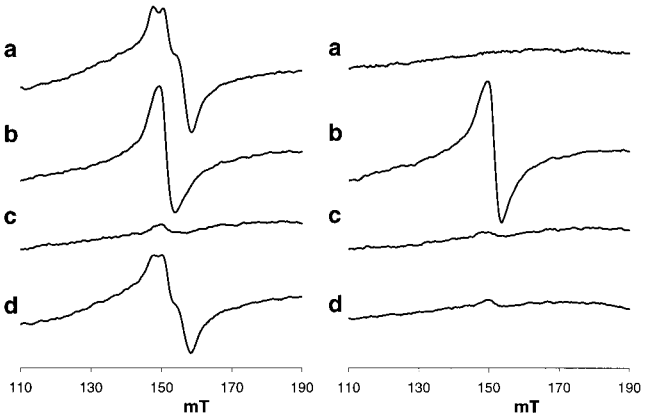

FIGURE 2: Separation of high and low molecular weight paramagnetic products after reaction of 6-OHDA with Fe-TF or $FeSO_4$. Left and right panels represent low-temperature EPR spectra recorded in solutions of Fe-TF (20 μM, 90% saturation) and $FeSO_4$ (40 μM), respectively. (a) Fe-TF or $FeSO_4$ in Tris buffer, 10 mM, pH 7.4; (b) same as "a" but after incubation with 6-OHDA (4 mM) for 2 h; (c) same as "b" but after filtration through 30 000 Da cutoff filters (volumes of samples were decreased 20-fold and restored with buffer before freezing for measurements). (d) same as "c", but CP and excess of $FeSO_4$ were added to the retentate. Instrumental settings were identical to those noted for Figure 1.

right, c). After filtration, the amplitude of signals from both solutions decreased 15−20-fold. Had the altered signal resulting from 6-OHDA treatment of Fe-TF resulted from TF modification, it would have been retained, and not lost, during filtration. In a parallel control study, the EPR spectrum of native Fe-TF did not change as a result of filtration (data not shown).

Finally, a combination of the two mechanisms—apoTF protein modification by generated oxygen radicals and iron binding by 6-OHDA oxidation products—may be responsible for the observed changes in the EPR spectra of Fe-TF incubated with 6-OHDA. One may assume that oxygen radical-induced modification of apoTF protein is irreversible such that any further binding of added iron by the modified protein will be unlikely. To this end, we attempted to regenerate Fe-TF (from apoTF) after treatment with 6-OHDA and monitor its EPR spectra. This, however, could not be done in the presence of 6-OHDA oxidation products that competitively bound iron and produced an EPR signal of the chelated iron in the spectrum. Therefore, more than 95% of the 6-OHDA oxidation products and iron released from Fe-TF were removed by filtration (through 30 000 Da cutoff filters), the retentate was readjusted to the initial volume with the same buffer, and $FeSO_4$ and CP were added to the retentate (in concentrations sufficient for saturation of equivalent amounts of untreated apoTF). The EPR spectrum of this "regenerated" Fe-TF was recorded (Figure 2, left, d). The shape of this spectrum was slightly different from that of the initial Fe-TF. It represented, most likely, superposition of two signals: one from Fe-TF and the other one from complexes of Fe(III) with residual (not completely removed by filtration) 6-OHDA oxidation products (Figure 2, right, d). Additional amounts of iron did not change either the shape or the magnitude of the EPR signal, suggesting that all available sites of TF were saturated with iron. Integration and analysis of the spectrum showed that almost 82% of the initial apoTF reacted with iron after exposure to 6-OHDA. Comparison of these data with the results of analysis of the

Table 1: Effect of 6-OHDA on the Fe-TF EPR Signal ($g = 4.3$)[a]

additions	Fe-TF EPR signal, % of total spectrum
Fe(III)-Q	3 ± 15
Fe-TF	103 ± 5
+6-OHDA, 30 min	74 ± 6
+6-OHDA, 1 h	62 ± 17
+6-OHDA, 2 h	20 ± 23
Fe-TF recovered	82 ± 6

[a] The intensity of $g = 4.3$ signals in EPR spectra was determined by their double integration. Both before and after treatment with 6-OHDA, the integral intensity of $g = 4.3$ signals did not significantly change. Treatment with 6-OHDA caused changes in the shape of the signal. Two signals were observed in these spectra: one resulting from release of iron and its reuptake by 6-OHDA oxidation products, the other one from residual Fe-TF. Numbers in the table represent the contribution of the Fe-TF signal to the total intensity of signals with $g = 4.3$. Analysis of the fractional contribution of the Fe-TF signal to the total intensity was performed using standards of pure Fe-TF and complexes of Fe(III) with 6-OHDA oxidation products prepared in the presence of the same amount of iron. Incubation conditions: $FeSO_4$ (40 μM) was incubated with 6-OHDA (4 mM) in Tris buffer, 10 mM, pH 7.4, for 2 h ["Fe(III)-Q"]. Fe-TF (20 μM) 90% saturated with iron ("Fe-TF") was incubated in the presence of 6-OHDA (4 mM) as indicated ("+6-OHDA, ..."). Fe-TF treated with 6-OHDA for 2 h was filtered through 30 000 Da cutoff filters, the retentate was readjusted to the initial volume with the buffer, and CP and excess $FeSO_4$ were added ("Fe-TF recovered").

EPR spectra of Fe-TF incubated with 6-OHDA for 2 h (Table 1) showed that about 20% of the Fe-TF signal might be irreversibly lost due to modification of the protein and was unrecoverable upon addition of $FeSO_4$. Thus, both modification of TF protein and release of iron from TF occur in the presence of 6-OHDA.

Chelation of Released Fe(II) by Ferrozine. Direct reduction of Fe(III) coordinated by TF is one possible mechanism for the latter reaction. In fact, even if the mechanism of iron release is not via its direct reduction, iron liberated by any mechanism will be readily reduced by 6-OHDA and/or superoxide formed obligatorily from it. This suggests that formation of Fe^{2+} should be observed, and that released iron could be removed from this chemical reaction by a specific chelator for Fe(II) like ferrozine. This is indeed the case. Incubation of Fe-TF with 6-OHDA in the presence of ferrozine facilitated detection of Fe(II) in the form of its ferrozine complex. This complex has a characteristic absorbance maximum at 560 nm (Figure 3A, 1) (*19*). Since 6-OHDA quinone also strongly absorbs at $\lambda_{max} = 488$ nm (Figure 3A, 2), formation of both of these species was observed in spectra of incubations containing Fe-TF, 6-OHDA, and ferrozine. In these spectra, the iron−ferrozine complex is seen as a shoulder on the quinone peak (Figure 3A, 3). In contrast, in the absence of 6-OHDA, the spectra of Fe-TF and ferrozine in solution did not change over time (Figure 3A, 4).

Incubation of Fe-TF with 6-OHDA in the presence of ferrozine had no effect on the shape of the Fe-TF signal in the EPR spectrum, but decreased the amplitude of the signal (Figure 3B) for Fe-TF with different levels of iron saturation (30, 60, and 90%). In each case, the signal amplitude dropped to 20−40% during a 2 h incubation with 6-OHDA and ferrozine.

Ascorbate Radical-Based Detection of Iron Recycling. In the presence of reductants, such as ascorbate, iron released

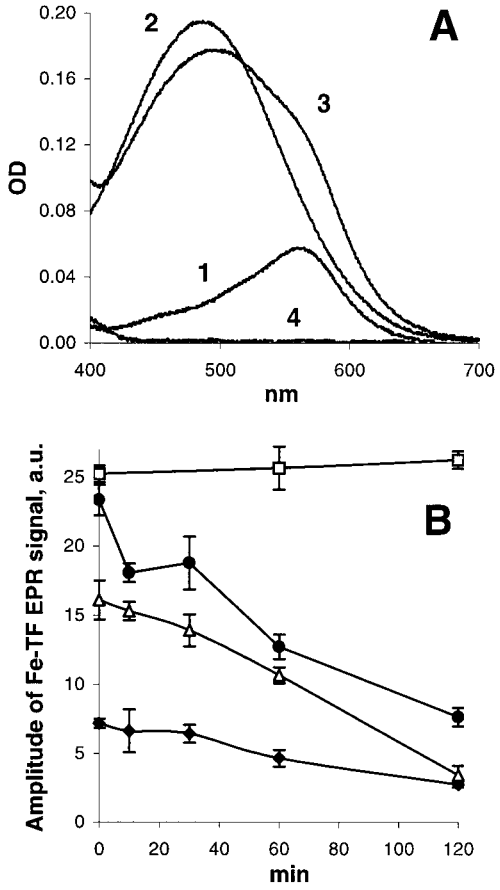

FIGURE 3: Fe(II)−ferrozine complex formation resulting from treatment of Fe-TF with 6-OHDA. (A) Optical spectra of *p*-quinone formed from 6-OHDA and Fe(II)−ferrozine complexes. 6-OHDA (4 mM), Fe-TF (20 μM, 90% saturation), and ferrozine (400 μM) were incubated in various combinations for 2 h and then diluted 12 times in a cuvette. (1) $FeSO_4$ (3.3 μM), ferrozine (200 μM) (final concentrations); (2) 6-OHDA; (3) 6-OHDA, Fe-TF, and ferrozine; (4) Fe-TF, ferrozine. (B) Time courses of the low-temperature EPR signal of Fe-TF (20 μM) in the presence of 6-OHDA (4 mM) and ferrozine (400 μM). Fe-TF was 90% (closed circles, open squares), 60% (open triangles), or 30% (closed diamonds) saturated with iron. Open squares represent the incubation system in the absence of 6-OHDA. Spectrometry conditions are as described under Figure 1.

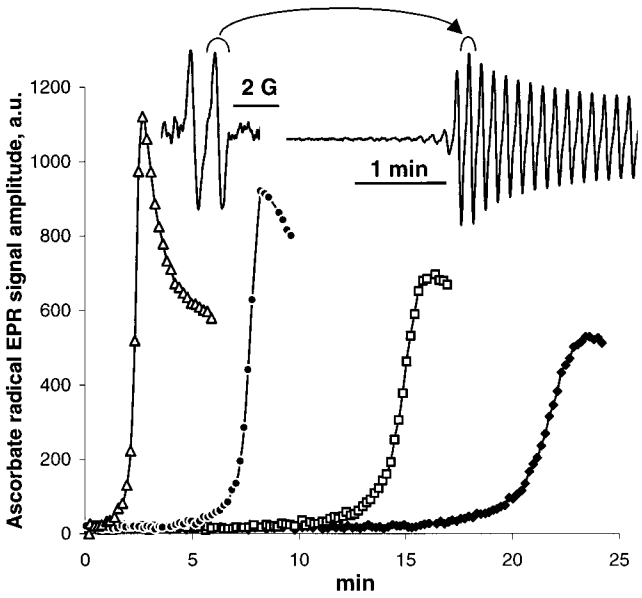

FIGURE 4: Time course of ascorbate radical generation by the Fe/6-OHDA/SOD system. Ascorbate (500 μM), SOD (10 μM), and 6-OHDA (500 μM) were incubated with $FeSO_4$ [5 μM (open triangles), 1 μM (closed circles), 0.2 μM (open squares)] or without iron (closed diamonds). The ascorbate radical EPR spectrum (inset, left) was recorded at the following settings: 335.4 mT, center field; 0.4 mT, sweep width; 0.063 mT, field modulation; 10 mW, microwave power; 0.1 s, time constant; 1 min, time scan. Time courses of ascorbate radical generation were obtained by repeated scanning of the magnetic field corresponding to the low-field peak of the EPR spectrum (inset, right). Instrumental conditions: 335.4 mT, center field; 0.15 mT, sweep width; 0.063 mT, field modulation; 10 mW, microwave power; 0.1 s, time constant; 10 s, time scan; internal mode of recording.

from Fe-TF can undergo redox cycling. We developed a very sensitive system for assay of redox-active iron based on ascorbate radical detection. In accord with previous results of Gee and Davison (*20*), we added SOD to the 6-OHDA solution (to inhibit superoxide-driven 6-OHDA oxidation) and monitored iron-induced formation of ascorbate radical from ascorbate. Production of ascorbate radical was measured by EPR in the repeated scanning mode of a single peak of the characteristic ascorbate doublet signal with $a^H = 1.7$ G (Figure 4, inset). In the presence of 6-OHDA, no signal was initially observed due to ascorbate radical reduction by this catechol. At the point in the time course when 6-OHDA was almost depleted (data not shown), the ascorbate radical EPR signal amplitude rose sharply. Both the signal amplitude and the inflection time of ascorbate radical generation were dependent on the iron concentration (Figure 4). The variation in inflection time is ascribed to catalytic 6-OHDA oxidation by iron; that is, the more iron, the faster oxidation. Addition of 6-OHDA-pretreated apoTF or Fe-TF to the ascorbate/SOD/6-OHDA system had opposite effects on the inflection time. Inflection time was increased by apoTF and decreased by Fe-TF (Table 2). The effect of 6-OHDA-pretreated 2.5 μM Fe-TF corresponded approximately to the effect of 1 μM free iron while untreated apoTF and Fe-TF caused

Table 2: Inflection Time of Ascorbate Radical Production in the SOD/6-OHDA System in the Presence of Treated and Untreated ApoTF or Fe-TF[a]

additions	inflection time (min)
OHDA	20.34 ± 0.75
OHDA + pretreated Fe	3.76 ± 0.42
OHDA + pretreated Fe-TF	9.22 ± 1.15
OHDA + pretreated apoTF	24.53 ± 0.44
OHDA + Fe-TF	17.82 ± 1.13[b]
OHDA + apoTF	21.91 ± 0.29[c]

[a] Fe-TF (25 μM, 85% saturated with iron), apoTF (25 μM), or Fe(II) (40 μm) were pretreated with 6-OHDA (4 mM) for 2 h. Immediately after treatment, samples were diluted 8-fold in a system designed for ascorbate radical measurement. This system contained ascorbate (500 μM), SOD (10 μM), and 6-OHDA (500 μM). Activities of untreated apoTF and Fe-TF were measured as controls. The inflection time of ascorbate radical generation was defined as the point on the time course at which the rate of increase of the EPR signal amplitude was maximal. CP (0.4 unit/mL) was present in all incubations to eliminate its interference with 6-OHDA oxidation. Time courses of ascorbate radical were obtained by repeated scanning of the magnetic field corresponding to the low-field peak of the spectrum. Instrumental conditions were as follows: 335.4 mT, center field; 0.15 mT, sweep width; 0.063 mT, field modulation; 10 mW, microwave power; 0.1 s, time constant; 10 s, time scan; internal mode of recording. [b] $p < 0.02$ vs samples incubated in the presence of OHDA alone ($n = 4-6$). [c] $p < 0.009$ vs samples incubated in the presence of OHDA alone ($n = 4-6$).

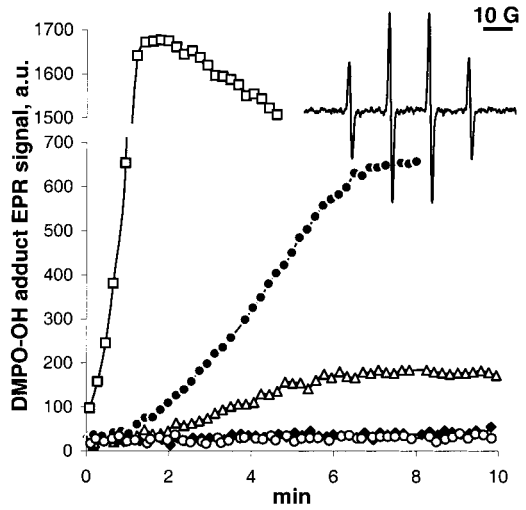

FIGURE 5: Effect of Fe, Fe-TF, and apoTF on DMPO-OH production in the presence of 6-OHDA. 100 mM DMPO and 500 μM 6-OHDA (open triangles) were incubated in Tris buffer (10 mM, pH 7.4) in the presence of 5 μM $FeSO_4$ (open squares), or in the presence of 2.5 μM Fe-TF 90% saturated with iron (closed circles), or 2.5 μM apoTF (closed diamonds), or 200 μM DFO (open circles). Time courses of DMPO-OH adduct generation were obtained by repeated scanning of the magnetic field corresponding to one of the peaks of the EPR spectrum under the following conditions: 333.2 mT, center field; 0.3 mT, sweep width; 0.1 mT, field modulation; 10 mW, microwave power; 0.1 s, time constant; 10 s, time scan; internal mode of recording.

statistically significant and opposite effects which, however, were very weak (Table 2).

Hydroxyl Radical Production by 6-OHDA and Fe-TF. The toxicological importance of iron recycling relates in part to its role in the production of hydroxyl radical. Hydroxyl radical is formed in solutions of 6-OHDA as a consequence of H_2O_2 generation and its reaction with released Fe(II). Hydroxyl radical was detected by EPR using the spin trap DMPO. DMPO forms stable adducts with $^{\bullet}$OH which have a characteristic EPR spectrum (Figure 5, inset) with hyperfine splitting constants of $a^N = 14.87$ G and $a^H = 14.81$ G (*21*). Open triangles in Figure 5 display the time course of DMPO-OH formation in Tris buffer in the presence of 6-OHDA alone. Upon addition of Fe(II), the rate of DMPO-OH production and its maximal concentration increased dramatically (open squares). Fe-TF, which carried an equivalent amount of iron, caused a similar but significantly less pronounced effect (closed circles). In contrast, apoTF and iron chelator, deferoxamine (DFO), blocked virtually all hydroxyl radical formation (closed diamonds and opened circles, respectively).

The observed generation of DMPO-OH adducts may be due to direct trapping of $^{\bullet}$OH radicals produced by the 6-OHDA/Fe system or, alternatively, due to reaction of iron with DMPO. To confirm production of $^{\bullet}$OH radicals, spin trapping by DMPO was performed in the presence of ethanol (50%) as a scavenger of $^{\bullet}$OH radicals or catalase that decomposes H_2O_2 and hence prevents $^{\bullet}$OH generation from H_2O_2. In the presence of ethanol, a six-line EPR spectrum of the DMPO adduct of $^{\bullet}CH(OH)CH_3$ ($a^N = 15.8$ G, $a^H = 23$ G) was observed instead of the DMPO-OH adduct when 6-OHDA/Fe and DMPO were incubated in phosphate buffer (50 mM). This confirms that highly reactive hydroxyl radical interacted with ethanol, yielding C-centered radical, as has been described earlier (*22*). Addition of catalase (10 units/mL) to the 6-OHDA/Fe system caused a drop in the amplitude of the DMPO-OH adduct EPR signal by an order of magnitude. The rate of DMPO-OH adduct decomposition, however, was considerably increased in the presence of catalase. It is likely that the peroxidase activity of catalase oxidized DMPO-OH adducts to EPR-silent nitrones as has been previously reported by Britigan and Hamill (*23*).

Effect of 6-OHDA on Fe-TF in Plasma. Aerobic incubation of human plasma (which contained the physiological 20−25% iron-saturated transferrin) with 6-OHDA did not cause a detectable change in the Fe-TF EPR signal (Figure 6, a, c). At the same time, oxidation of 6-OHDA (quinone formation) was even faster in plasma than in buffer (data not shown). It appears as if these two processes (6-OHDA oxidation and Fe release) were completely uncoupled in plasma. It should be noted that 6-OHDA oxidation is promoted by superoxide and can be catalyzed by CP (*13*). The concentration of CP in plasma ($\sim$300 μg/mL) is 60 times higher than in our model system. Theoretically, CP may oxidize 6-OHDA without superoxide production and may do so more efficiently from the point of view of oxygen consumption ($O_2 + 4H^+ - 4e \rightarrow 2H_2O$) (*24*). Furthermore, CP has ferroxidase activity and facilitates reuptake of iron by TF (*25, 26*).

All of these reactions require oxygen. We therefore studied the effect of oxygen on the modulation of the EPR signal of Fe-TF by 6-OHDA. Samples exposed to each of three different plasma O_2 saturation conditions were studied during a 1.5 h incubation with 6-OHDA. Conditions examined were as follows: in equilibrium with air, under flow of 100% oxygen, and under N_2 flow (Figure 6, b, c, and d, respectively). No changes in either profile or magnitude of the Fe-TF EPR signal were observed when plasma was incubated with 6-OHDA under aerobic conditions or in pure oxygen. The effect of 6-OHDA on the Fe-TF EPR signal in plasma under N_2 was similar to that seen in Tris buffer. In both cases, two effects of 6-OHDA on EPR signals were observed. The shape of the signal changed and the intensity of the signal (evaluated by its double integration) decreased after 6-OHDA treatment. Loss of signal intensity is likely associated with decomposition of Fe-TF complexes. Changes of the signal shape are manifest of new paramagnetic species likely to be complexes of Fe(III) with 6-OHDA oxidation products. We observed a pronounced (50−70%) decrease in intensity of the EPR signal in plasma under N_2 relative to that seen before 6-OHDA treatment. Changes in the shape of the signal were minimal under N_2 flow (Figure 6, d). (It should be noted, however, that using nitrogen flow, we were not able to fully exclude oxygen from the system and completely avoid formation of complexes of iron with 6-OHDA oxidation products.) In contrast, dramatic 6-OHDA-induced changes in the shape of the EPR signal were detected in model systems in vitro under aerobic conditions (Figure 1). These were accompanied by only slightly decreased (by 20−30%) signal intensity of Fe-TF. Thus, decomposition of Fe-TF complexes seems to be mainly responsible for the observed 6-OHDA-induced changes in the EPR signal of plasma under N_2 while both decomposition of Fe-TF complexes and subsequent chelation of released iron by 6-OHDA oxidation products were likely involved in EPR spectral changes in vitro under aerobic conditions.

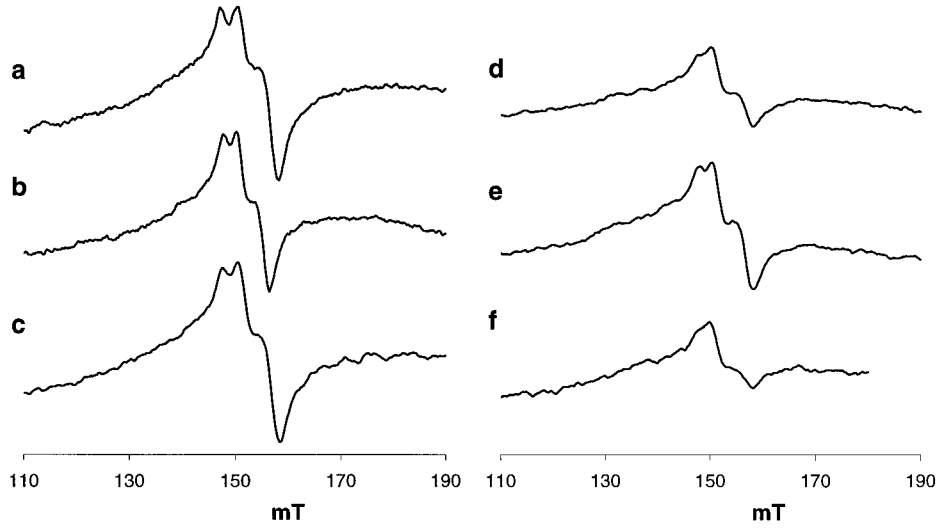

FIGURE 6: Effect of 6-OHDA on the low-temperature EPR signal of transferrin in human plasma. Incubation conditions: plasma control (a); plasma with 6-OHDA (4 mM): in equilibrium with air (b) or under flow of pure O_2 (c); plasma under flow of N_2: plus 6-OHDA (4 mM) (d); same as "d" plus TEMPOL (5 mM) (e); same as "d" plus SOD (10 μM) (f). All incubations were carried out for 1.5 h. Plasma was partially evaporated during incubation, and its volume was restored with Tris buffer, 10 mM, pH 7.4, exposed to the same flow of gas as the original sample. Instrumental conditions are the same as described under Figure 1.

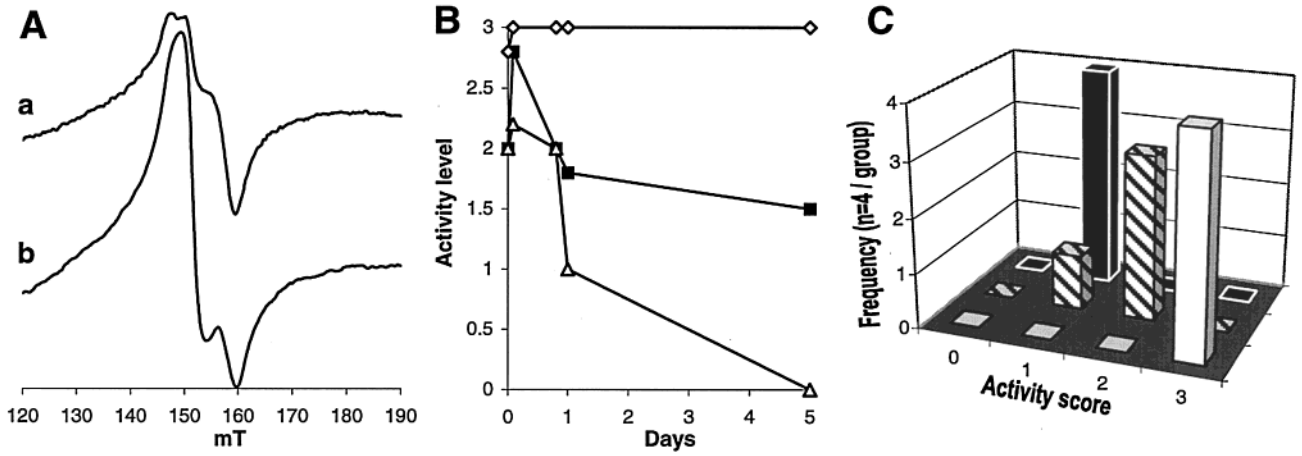

FIGURE 7: Evidence for iron release from transferrin in 6-OHDA-treated mice. (A) Representative low-temperature EPR signal of transferrin in blood obtained from male A/J mice (5−7 weeks old) 1 h after treatment with saline (a) or 6-OHDA (b; 350 mg/kg) by intraperitoneal injection. Instrumental conditions are the same as described under Figure 1. (B) Male A/J mice (5−7 weeks old) were administered deferioxamine (DFO; 130 mg/kg) or saline by intraperitoneal injection. Two hours later, 6-OHDA (350 mg/kg) or saline was administered. An activity level was assigned to each mouse at various time points as we have previously described (*3*, *4*) as a measure of systemic well-being. Plotted values represent the mean for each group ($n = 4$) at each time point: DFO + saline (diamonds), DFO + 6-OHDA (squares), saline + 6-OHDA (triangles). All mice in all groups had activity levels of 3 prior to injection of 6-OHDA ($t = -0.01$ h). Measurements taken at $t = 0$ represent determinations made immediately following i.p. injection of 6-OHDA. The deviation of the activity level from 3 immediately after injection and its rapid return to 3 in mice treated with DFO + saline are not significantly different from those seen in mice treated with i.p. saline alone (data not shown). Standard errors are not plotted, as the activity level is a semiquantitative, nonparametric measure. However, values plotted for DFO + 6-OHDA differ from those for saline + 6-OHDA with $p < 0.02$ at 1 day and <0.04 at 5 days after 6-OHDA injection (Mann−Whitney U test). In addition, a histogram of the distribution of possible activity levels in each of the groups on day 1 after 6-OHDA injection (C) demonstrates that they represent three distinct populations (white bars, DFO + saline; gray bars, DFO + 6-OHDA; black bars, saline + 6-OHDA).

Thus, 6-OHDA is still able to release iron from TF in plasma. However, our ability to detect this release by low-temperature EPR spectroscopy is most likely hampered by the ferroxidase activity of plasma and the high rate of catechol oxidation in the presence of relatively high oxygen concentrations. We attempted to reproduce both "protective" activities of plasma against 6-OHDA-induced iron release from Fe-TF under N_2 using the stable nitroxide radical 2,2,6,6-tetramethylpiperidine-1-oxyl (TEMPOL). TEMPOL has been reported to possess ferroxidase activity (*27*), and, most importantly, oxidize 6-OHDA directly (*4*). In addition, the nitroxide radical acts as an SOD mimic (*28*). We found that TEMPOL (5 mM), indeed, was able to prevent 6-OHDA-induced iron release from Fe-TF in plasma under nitrogen (Figure 6, e). The Fe-TF EPR signal decreased only by 20−30% and was not changed in shape when TEMPOL was added to the solution. SOD did not have any effect on the Fe-TF signal under N_2 (Figure 6, f).

Effect of 6-OHDA on Murine Fe-TF in Vivo. Low-temperature EPR determinations on the blood of control mice administered saline (i.p.) 1 h earlier revealed a strong signal at $g = 4.3$ which represents Fe-TF (Figure 7, A, a). The shape of this signal was similar overall to that of Fe-TF in human plasma. As shown in Figure 7 (A, b), determination

of the low-temperature EPR signal of Fe-TF in blood from animals treated with 6-OHDA (350 mg/kg, i.p.) 1 h earlier reveals a dramatic change in the shape of this spectrum analogous to that seen for human TF in Tris buffer. This spectrum reflects the presence of a combination of high-spin Fe(III) both bound and unbound to TF. Of further interest, the signal after 6-OHDA administration was twice the amplitude of that of control mice. This reflects a doubling of the non-heme iron concentration in the blood of treated mice. There are two possible explanations for this latter finding: (1) non-heme iron is released to the extracellular compartment from disrupted cells; or (2) circulatory water volume (i.e., dilution of non-heme iron) decreases.

To distinguish between these two explanations, the hemoglobin concentration of the blood was determined in control and treated mice, and was found to be 1.5 times higher in the latter than in the former animals. Blood samples were frozen in liquid nitrogen to disrupt erythrocytes. Hemolyzed blood was diluted by 1500-fold in Tris-HCl buffer, and the optical density at 414 nm was measured. The mean OD_{414} values were 0.62 ± 0.04 before treatment and 0.93 ± 0.07 1 h after treatment, respectively ($n = 3$, $p = 0.002$, *t*-test). This is indirect evidence for contraction of the intravascular water volume. On this assumption, we determined the amount of iron released from Fe-TF. Expansion of the EPR spectra representing Fe-TF and Fe(III) unbound to transferrin, respectively, revealed that TF had released at least 40% of its bound iron at 1 h after 6-OHDA treatment.

Protective Effect of DFO in Mice Treated with 6-OHDA. To test our hypothesis that iron plays a role in the toxicity of 6-OHDA in vivo, we administered 6-OHDA (350 mg/kg) to mice intraperitoneally 2 h after injection of either saline or DFO (130 mg/kg) dissolved in saline, and observed the mice over the ensuing several days. As is shown in Figure 7B, mice pretreated with DFO exhibited less systemic toxicity of 6-OHDA than did those pretreated with saline as a control ($p < 0.02$ at 24 h and $p < 0.04$ at 5 days after 6-OHDA injection; Mann−Whitney U test). The statistical and biological significance of these data are underscored by the histogram in Figure 7C showing that by 1 day after 6-OHDA injection, animals treated with saline followed by 6-OHDA, DFO followed by 6-OHDA, or DFO followed by saline constitute three distinct populations relative to three biologically disparate possible outcomes. This effect remains robust at 5 days after treatment (histogram not shown).

DISCUSSION

Treatment of Fe-TF with 6-OHDA results in the release of iron from this complex. The present studies demonstrate that this reaction is important even at physiological levels of iron saturation. There are three possible biochemical mechanisms of iron release: reduction of Fe(III) by 6-OHDA, reduction by $O_2^{\bullet-}$, or release resulting from protein damage by $^{\bullet}OH$. While all of them may contribute to iron release from Fe-TF under aerobic conditions, the results of our studies with plasma in the absence of oxygen are most consistent with the first of these mechanisms.

In any case, the iron thus released would further enhance oxidation of 6-OHDA, and therefore the production of $O_2^{\bullet-}$, H_2O_2, and $^{\bullet}OH$ via the Fenton reaction. These species would in turn perpetuate the release of iron from TF. This redox cycling process may be further enhanced by interaction of released iron with endogenous reductants, such as ascorbate, yielding even greater amplification of oxygen radical production. As might be expected, 6-OHDA oxidation and hydroxyl radical production were hastened in the presence of subsaturated Fe-TF.

We propose that similar reactions are operative in the bloodstream in vivo. The in vivo case is, however, somewhat more complex and involves other oxygen-dependent processes as well. Those mediated by the ferroxidase activity of plasma, oxidation of 6-OHDA by O_2 and $O_2^{\bullet-}$, and catalytic 6-OHDA oxidation by CP might contribute to the ultimate availability of iron from Fe-TF. Ferroxidase activity would result in reuptake of Fe by TF and reduce the availability of iron to produce $^{\bullet}OH$ via Fenton chemistry. Oxidation of 6-OHDA by O_2 and $O_2^{\bullet-}$ or indirectly by CP would decrease the probability of subsequent interaction between Fe-TF and 6-OHDA. The concentration of CP in our model systems was 20−60 times lower than that of human plasma. This may explain the difference in effect of 6-OHDA on the Fe-TF EPR signal between solutions in buffer and plasma under air. In support of this notion, removing oxygen, a necessary substrate for CP activity, from plasma afforded detection of the change in the Fe-TF EPR signal produced by 6-OHDA.

It is important to note that the concentration of "free" oxygen in human venous blood ranges from 5 (normal oxygenation) to 20 (severe hypoxia) times lower than that of solutions equilibrated with air. In the present study, the effect of 6-OHDA was tested in two extreme conditions: in equilibrium with air (much higher O_2 concentration than physiologic) and under N_2 flow (much lower O_2 concentration than physiologic). The Fe-TF EPR signal was altered by 6-OHDA only under N_2. It is quite possible that in the circulation, the amount of "free" iron depends greatly on the O_2 and 6-OHDA concentrations. Iron liberation and resulting oxygen radical generation would be expected to occur in plasma with physiological levels of O_2 unless the oxidative activity of CP is sufficiently high to prevent it.

In support of this notion, we demonstrate identical changes in the Fe-TF signal in blood from 6-OHDA-treated mice to those seen in Tris buffer. We further demonstrate that in vivo pretreatment of mice with DFO, an iron chelator, protected them from the systemic effects of 6-OHDA. These two studies underscore the physiological and pharmacological relevance of the in vitro studies presented herein. We have previously found that it requires 6-OHDA doses as high as 350 mg/kg to prevent neuroblastoma tumor formation from subcutaneous microscopic implants of neuroblastoma in our animal model of "microscopic residual disease", the usual reason for failure of chemotherapy in children with neuroblastoma (*4*). The volume contraction that results with this dose probably results at least in part from dysautonomic diarrhea in these animals (Schor, unpublished observations), and relates to the sustained weight loss seen in neonatal animals sympathectomized with 6-OHDA (*29*). It is for this reason that treatment with 6-OHDA alone would almost certainly be untenable in children with neuroblastoma (*3*, *4*). Adjunctive treatment with agents such as DFO has therefore been proposed. DFO has been shown to have antineoplastic, differentiation-inducing effects on neuroblatoma cells (*30*), as well. Whether or not both safety and efficacy

could be achieved with adjunctive treatment depends at least in part on the degree to which DFO decreases 6-OHDA efficacy against neuroblastoma cells relative to its toxicity to other cellular and extracellular elements.

The present studies also suggest that DFO may be a useful drug in the prevention and slowing of progression of other disorders, like Parkinson's disease, that result from catechol-mediated oxygen radical generation. As is the situation for treatment of any chronic disease, institution of prophylactic therapy would require careful consideration of the long-term toxicity of the agent to be used, the risks of not instituting treatment and likelihood of efficacy of each drug, and the availability of other perhaps less toxic agents for the condition.

ACKNOWLEDGMENT

We are indebted to Karen D. Nylander for expert technical assistance.

REFERENCES

1. Jenner, P., and Olanow, C. W. (1996) *Neurology 47 (Suppl 3)*, 161−170.
2. Chelmicka-Szorc, E., and Arnason, B. G. (1976) *Cancer. Res. 36*, 2382−2384.
3. Schor, N. F. (1987) *Cancer Res. 47*, 5411−5414.
4. Purpura, P., Westman, L., Will, P., Eidelman, A., Kagan, V. E., Osipov, A. N., and Schor, N. F. (1996) *Cancer Res. 56*, 2336−2342.
5. Cohen, G., and Heikkila, R. E. (1974) *J. Biol. Chem. 249*, 2447−2452.
6. Monteiro, H. P., and Winterbourn, C. C. (1989) *Biochem. Pharmacol. 38*, 4177−4182.
7. Gee, P., and Davison, A. J. (1984) *Arch. Biochem. Biophys. 231*, 164−168.
8. Jeffrey, P. D., Bewley, M. C., MacGillivray, R. T., Mason, A. B., Woodworth, R. C., and Baker, E. N. (1998) *Biochemistry 37*, 13978−13986.
9. Kretchmar, S. A., Graig, A., and Raymond, K. N. (1993) *J. Am. Chem. Soc. 115*, 6758−6764.
10. Baldwin, D. A., Jenny, E. R., and Aisen, P. J. (1984) *J. Biol. Chem. 259*, 13391−13394.
11. Aruoma, O. I., and Halliwell, B. (1987) *Biochem. J. 241*, 273−278.
12. Minetti, M., Forte, T., Soriani, M., Quaresima, V., Menditto, A., and Ferrari, M. (1992) *Biochem. J. 282*, 459−465.
13. Medda, R., Calabrese, L., Musci, G., Padiglia, A., and Floris, G. (1996) *Biochem. Mol. Biol. Int. 38*, 721−728.
14. Bali, P. K., and Harris, W. R. (1990) *Arch. Biochem. Biophys. 281*, 251−256.
15. Sachs, A., and Johnson, G. (1975) *Biochem. Pharmacol. 24*, 1−8.
16. Siegel, S. (1956) *Nonparametric Statistics*, McGraw-Hill, New York.
17. He, Q. Y., Mason, A. B., Woodworth, R. C., Tam, B. M., MacGillivray, R. T., Grady, J. K., and Chasteen, N. D. (1997) *Biochemistry 36*, 14853−14860.
18. Linert, W., Herlinger, E., Jameson, R. F., Kienzl, E., Jellinger, K., and Youdim, M. B. (1996) *Biochim. Biophys. Acta 1316*, 160−168.
19. Stookey, L. L. (1970) *Anal. Chem. 42*, 779−781.
20. Gee, P., and Davison, A. J. (1989) *Free Radical Biol. Med. 6*, 271−284.
21. Rosen, G. M., and Rauckman, E. J. (1984) *Methods Enzymol. 105*, 198−209.
22. Finkelstein, E., Rosen, G. M., and Rauckman, E. J. (1980) *Arch. Biochem. Biophys. 200*, 1−16.
23. Britigan, B. E., and Hamill, D. R. (1989) *Arch. Biochem. Biophys. 275*, 72−81.
24. Messerschmidt, A., Huber, R., and Ryden, L. G. (1990) *Eur. J. Biochem. 187*, 341−52.
25. Ryden, L. (1984) in *Copper Proteins and Copper Enzymes* (Lontie, R., Ed.) Vol. III, pp 37−100, CRC Press, Boca Raton, FL.
26. Osaki, S., Johnson, D. A., and Frieden, E. J. (1966) *J. Biol. Chem. 241*, 2746−2751.
27. Mitchell, J. B., Samuni, A., Krishna, M. C., DeGraff, W. G., Ahn, M. S., Samuni, U., and Russo, A. (1990) *Biochemistry 29*, 2802−2807.
28. Krishna, M. C., Grahame, D. A., Samuni, A., Mitchell, J. B., and Russo, A. (1992) *Proc. Natl. Acad. Sci. U.S.A. 89*, 5537−5541.
29. Fink, D. W., Jr., and Mirkin, B. I. (1987) *Cancer Res. 47*, 5620−5625.
30. Iyer, J., Korones, D. N., Ikegaki, N., Kennett, R. H., and Frantz, C. N. (1991) *Prog. Clin. Biol. Res. 366*, 55−64.

BI992296V